Acceleration-field calculation for a structure-based laser-driven linear accelerator

Y. C. Huang[a)]
Department of Atomic Science, National Tsinghua University, Hsinchu, Taiwan 30043

R. L. Byer
Department of Applied Physics, Stanford University, Stanford, California 94305-4055

(Received 16 February 1998; accepted for publication 16 April 1998)

A laser-driven particle accelerator, scaled to optical wavelengths, has a feature size many orders of magnitude smaller than a radio-frequency accelerator. However, similar to a radio-frequency accelerator, a laser-driven accelerator cell may have apertures to transmit electrons. We numerically calculate the acceleration field for a cylindrically focused, crossed-laser-beam linear accelerator with the presence of electron transit apertures. A 4-μm-width electron aperture decreases electron energy gain by 17%, and a 6-μm-width aperture decreases energy gain by 34% relative to a structure without apertures. © *1998 American Institute of Physics.* [S0034-6748(98)02107-8]

I. INTRODUCTION

The much shorter wavelength of a laser-driven linear accelerator, compared to a radio-frequency (rf) microwave-driven accelerator, promises to provide increased acceleration gradients[1,2] and ultrashort electron bunches. High-gradient operation leads to compact, high-energy electron accelerators, whereas short electron bunches help to generate coherent, spontaneous radiation in the short wavelength regime. Consequently laser accelerators could be the ideal drivers for future ultracompact, high-brightness x-ray lasers.[3]

Structure-based accelerators may have electron transit apertures to transmit electrons from one accelerator cell to another. In a rf accelerator, where the operation wavelength is on the order of a centimeter, the electron aperture can be made small compared to rf wavelengths. As a result, little rf power radiates through the aperture at the end of the acceleration section. On the other hand, in a laser-driven accelerator, laser fields can leak through a micron-size electron aperture due to the short laser wavelength. The leakage fields interact with electrons and may lead to a decrease in electron energy gain.

In an accelerator, electrons gain or lose energy from vector electric fields. To derive an acceleration field from a linearly polarized laser beam, Edighoffer[4] *et al.* proposed to send electrons at an angle with respect to the laser beam axis. To cancel the transverse force on electrons, Haaland[5] proposed a symmetric configuration consisting of two properly phased laser beams, and Sprangle[6] *et al.* provided a satisfactory solution to the acceleration field without the presence of electron transit apertures. In an effort to realize the crossed-laser-beam accelerator, Huang and Byer[1] proposed a dielectric-based accelerator structure that is suitable for both spherical laser focusing and cylindrical laser focusing.[2] Since the cylindrical laser focusing scheme is superior in terms of structure fabrication, thermal loading, and high current operation,[2] we limit our discussion in this article to cylindrical laser focusing. We first present an analytic solution for the acceleration field in the proposed laser-driven accelerator without field disturbance from electron transit apertures. We then explore the effects of apertures through numerical calculations.

II. ACCELERATION FIELDS WITHOUT ELECTRON TRANSIT APERTURES

A simplified picture for the proposed laser-driven acceleration scheme is depicted in Fig. 1, where an electron traverses the focal zone of two crossed laser beams. In the figure the dashed lines designate Gaussian laser field profiles, the solid lines with arrows indicate the direction of laser beam propagation, and the cross-hatched areas are dielectric high reflectors. The two laser beams are phased such that the transverse fields cancel and the longitudinal fields add along the z axis. The inset in the figure defines the coordinate systems used in the article. The unprimed coordinate system includes the electron axis. The primes indicate the rotated laser beam coordinate system. The structure and the laser fields are constant in y for the cylindrically focused crossed-laser beams.

With no field variation in the y direction, the free-space electrical field in the x' direction for a fundamental Gaussian laser beam in phasor notation is given by[7]

$$\tilde{E}_{x'}=\left(\frac{2}{\pi}\right)^{1/4}\sqrt{\frac{2\eta}{w(z')}P_y}\exp\left[-jkz'+j\frac{\Phi(z')}{2}-j\frac{kx'^2}{2R(z')}+j\phi-\frac{x'^2}{w^2(z')}\right], \tag{1}$$

where P_y is the optical power per unit length in y, $\eta=377\ \Omega$ is the vacuum wave impedance, $k=2\pi/\lambda$ is the free-space wave number, $w(z')=w_0\sqrt{1+z'^2/z_r^2}$ is the $1/e$ laser field radius at z', w_0 is the laser waist defined at $z'=0$, $z_r=\pi w_0^2/\lambda$ is the optical Rayleigh range,[8] $R(z')=z'$

[a)]Electronic mail: ychuang@faculty.nthu.edu.tw

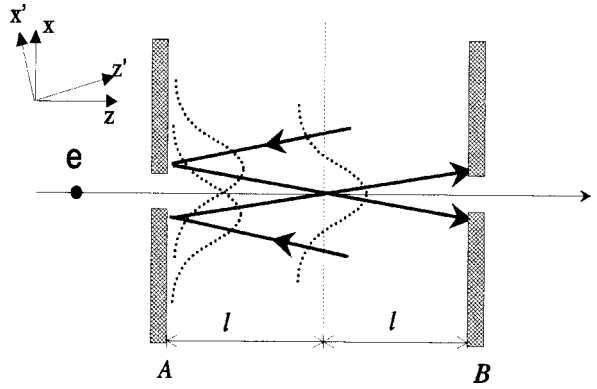

FIG. 1. The configuration for the crossed-laser-beam linear accelerator. The two laser beams are phased such that the transverse fields cancel and the longitudinal fields add along the z axis. The cross-hatched areas designate dielectric high reflectors. The primes indicate the rotated laser coordinates. The structure and the laser fields are constant in y so that the electron transit aperture is a slit along the y axis.

$+z_r^2/z'$ is the radius of curvature of the laser wavefront at z', $\Phi(z')=\tan^{-1}(z'/z_r)$ is the Guoy phase[9] due to diffraction, and ϕ is the electron entrance phase.

The electrical field component in z' can be calculated according to the Gauss law $\nabla' \cdot \mathbf{E}=0$ in a source-free region. In the paraxial approximation,[10]

$$\tilde{E}_{z'} \approx \frac{-j}{k}\frac{\partial \tilde{E}_{x'}}{\partial x'} = \tilde{E}_{x'} \cdot \left[\frac{-x'}{R(z')} + 2j\,\frac{x'}{kw^2(z')}\right]. \tag{2}$$

Summing the z component fields from $\tilde{E}_{z'}$ and $\tilde{E}_{x'}$ with appropriate coordinate transformation, we show in Ref. 2 the axial acceleration field is given by

$$E_z = -2\sqrt{2\eta I_{\max}}\cdot\theta\cdot\frac{(1+\hat{l}^2)^{1/4}}{(1+\hat{z}^2)^{3/4}} \times \exp\left(\frac{-\hat{z}^2\hat{\theta}^2}{1+\hat{z}^2}\right)\cos\left(\frac{\hat{z}\hat{\theta}^2}{1+\hat{z}^2}+1.5\tan^{-1}\hat{z}\right), \tag{3}$$

where $\hat{z}\equiv z/z_r$ is the normalized z coordinate, $\hat{z}=0$ is chosen at the geometric center of the structure, $\hat{\theta}\equiv\theta/\theta_d$ is the laser crossing angle θ normalized to the laser far-field diffraction angle[11] $\theta_d \equiv w_0/z_r$, and $I_{\max}$ is the maximum laser intensity that the dielectric high reflector may sustain at $\hat{z}=\hat{l}$. In deriving Eq. (3), we assume a small crossing angle $\theta \ll 1$, a large electron energy $\gamma \gg 1/\theta$ (γ is the relativistic factor), and zero phase slip at $z=0$. The small angle approximation reduces phase slip as indicated in the phase term of Eq. (3).

Figure 2 shows the axial acceleration field profile and electron phase slip versus distance for $\theta=50$ mrad, $w_0=25\ \mu$m, $\lambda=1\ \mu$m, and $I_{\max}=20$ TW/cm^2 for 100 fs laser pulses.[12] For this particular design, the phase slip resulting from the Guoy phase term and the laser crossing angle gives an acceleration distance much shorter than a Rayleigh range. For an interaction length of $2l=340\ \mu$m, the proposed structure gives ~ 0.7 GeV/m average acceleration gradient over the whole length of the accelerator.[2]

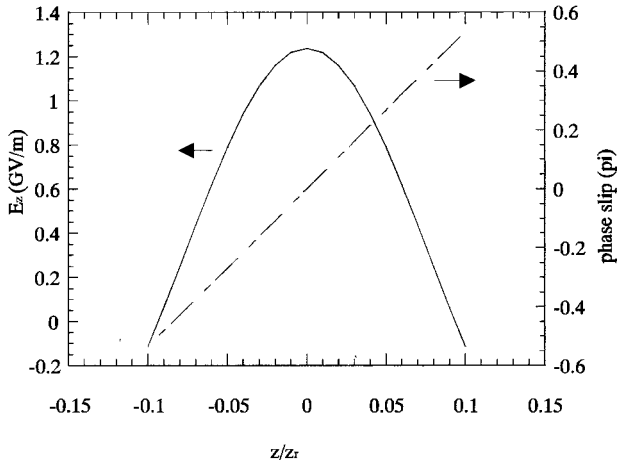

FIG. 2. The axial acceleration field profile and electron phase slip angle versus distance. The design parameters are: laser crossing angle $\theta=50$ mrad, laser waist size $w_0=25\ \mu$m, laser wavelength $\lambda=1\ \mu$m, and laser damage intensity $I_{\max}=20$ TW/cm^2 for 100 fs laser pulses. For this particular design, the π phase slip between $|z/z_r|<0.1$, where $z_r=1.96$ mm, resulting from the Guoy phase term and the laser crossing angle, gives an acceleration distance $\sim 0.2z_r=0.39$ mm much shorter than a Rayleigh range.

III. ACCELERATION FIELDS WITH ELECTRON TRANSIT APERTURES

As shown in Fig. 1, the leakage laser fields at the entrance aperture reduce the acceleration field inside the accelerator cell. Similarly, at the exit aperture, the leakage laser fields continuously interact with electrons until the laser fields diffract to a negligible level.

Classical diffraction theories such as Fresnel diffraction and Fraunhofer diffraction, approximated from the Kirchhoff and Rayleigh–Sommerfeld formalisms, deal with scalar fields. Furthermore the classical theories fail when (1) the diffraction aperture size is comparable to the radiation wavelength, and (2) the field is observed near the aperture.[13] To contain the laser field and achieve acceleration, the proposed accelerator has a transit aperture larger than the pumping wavelength and operates in the near-field region. Therefore we must take into account the diffracted vector fields caused by the apertures in the near-field region.

A plane-wave solution satisfies Maxwell's equations everywhere. With known boundary conditions, it is possible to synthesize the vector components of an arbitrary, two-dimensional, electromagnetic wave by superimposing many plane waves.[4] Specifically an arbitrary vector field component $\tilde{E}_x(x,z)$ can be expressed as

$$\tilde{E}_x(x,z) = \int_{-\pi/2}^{\pi/2} a(\theta)\cos\theta \times \exp(-jkx\sin\theta - jkz\cos\theta)\,d\theta, \tag{4}$$

and the corresponding $\tilde{E}_z(x,z)$ of the wave is

$$\tilde{E}_z(x,z) = \int_{-\pi/2}^{\pi/2} a(\theta)\sin\theta \times \exp(-jkx\sin\theta - jkz\cos\theta)\,d\theta. \tag{5}$$

As long as the angular spectrum $a(\theta)$ is known, derived from a known boundary condition $\tilde{E}_x(x,z=0)$, the vector fields $\tilde{E}_x(x,z)$ and $\tilde{E}_z(x,z)$ everywhere in space can be determined from Eqs. (4) and (5). For our numerical calculation, we arbitrarily set $z=0$ at the aperture boundaries. The boundary condition $\tilde{E}_x(x,z=0)$ can be obtained from the sum of the two crossed Gaussian beams with a zero field across the aperture at the entrance (boundary A in Fig. 1) or across the dielectric at the exit (boundary B in Fig. 1). This approximation gives hard-edged discontinuities at the slit edges.

In theory the angular spectrum $a(\theta)$ must be within $-\pi/2 \leqslant \theta \leqslant \pi/2$. To simplify the numerical calculation, we write $\tilde{E}_x(x,z=0)$ and a temporary function $A(\theta)$ into Fourier transform pairs, given by

$$A(\theta)=\int_{-\infty}^{\infty}\tilde{E}_{x,h}(x,z=0)\times\exp(+jkx\ \sin\ \theta)d(x/\lambda), \tag{6}$$

$$\tilde{E}_{x,h}(x,z=0)=\int_{-\infty}^{\infty}A(\theta)\exp(-jkx\ \sin\ \theta)d\ \sin\ \theta, \tag{7}$$

where the index h in $\tilde{E}_{x,h}(x,z=0)$ designates the x-component electric field from the hard-edged boundary condition. After obtaining $A(\theta)$ from Eq. (7), we then truncate $A(\theta)$ at $\theta=\pm\pi/2$ to approximate $a(\theta)$. The thus-obtained $a(\theta)$ is used to calculate the acceleration field $\tilde{E}_z(x,z)$ from Eq. (5), and gives a modified boundary field $\tilde{E}_{x,m}(x,z=0)=\int_{-\pi/2}^{\pi/2}A(\theta)\exp(-jkx\sin\theta)\cos\theta d\theta$. The legitimacy of this numerical technique requires that $\tilde{E}_{x,m}(x,z=0)$ be close to $\tilde{E}_{x,h}(x,z=0)$, which is indeed the case in our parameter range. Since the laser crossing angle is small for our design, the values of $A(\theta)$ outside $\theta=\pm\pi/2$ are primarily contributed from the hard-edged boundary field $\tilde{E}_{x,h}(x,z=0)$. Typically diffraction at a small aperture at the accelerator boundary yields high spatial frequencies, which tend to spread for values of $A(\theta)$ outside $\theta=\pm\pi/2$. The truncated $A(\theta)$ results in an oscillatory $\tilde{E}_{x,m}(x,z=0)$ near the aperture edges.

Figure 3 shows the comparison between the x-component electric field $E_x(x,z=0)$ with no aperture (curve a), and $E_{x,m}(x,z=0)$ with a 4 μm aperture (curve b) at the accelerator entrance A. The design parameters are $\theta=50$ mrad, $w_0=25$ μm, and $\lambda=1$ μm. As can be seen, the truncated $A(\theta)$ gives an $E_{x,m}(x,z=0)$ that oscillates slightly near the slit boundaries, but overlaps very well with $E_x(x,z=0)$ everywhere else. In practice, the high reflection coatings on dielectric cannot be perfect at the aperture edges. The smoothed boundary field resulting from the truncated $A(\theta)$ might be in fact closer to real situations.

Once $a(\theta)$ is calculated, the x-component electric field immediately before the boundary B in Fig. 1 can be obtained from Eq. (4). Repeating the same procedures for calculating $\tilde{E}_z(x,z)$ inside the accelerator cell, one may solve $\tilde{E}_z(x,z)$ outside the boundary B.

Single-stage electron energy gain can be obtained by integrating the acceleration field $\tilde{E}_z(x,z)$ along z. Figure 4 plots the electron energy gain versus distance with zero, 4

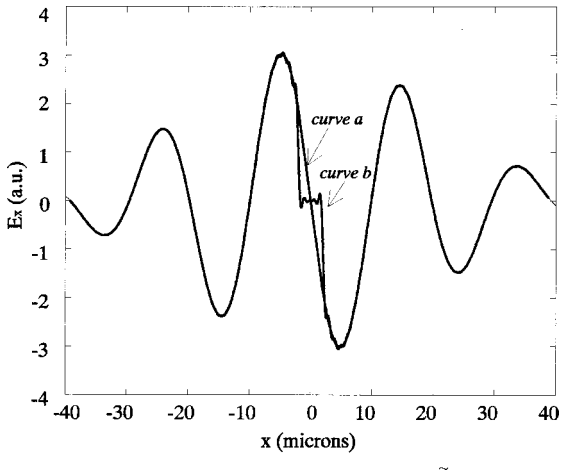

FIG. 3. Comparison between the x-component electric field $\tilde{E}_x(x,z=0)$ with no electron aperture (curve a) and the modified $\tilde{E}_{x,m}(x,z=0)$ with a 4 μm aperture (curve b) at the accelerator entrance. The design parameters are $\theta=50$ mrad, $w_0=25$ μm, and $\lambda=1$ μm. The modified boundary field $E_{x,m}(x,z=0)$ oscillates slightly near the slit boundaries, but overlaps very well with the $E_x(x,z=0)$ everywhere else.

μm and 6 μm slit apertures. The system parameters are $\theta=50$ mrad, $w_0=25$ μm, $\lambda=1$ μm, and the interaction length is $2l=340$ μm. Again zero phase slip is assumed at the center of the accelerator structure. Without the electron apertures, the electron retains its energy gain after exiting the accelerator cell at B; whereas with the apertures the electron sees a slightly phase-mismatched field at the entrance A and loses a fraction of its energy gain to the leaking laser field after B. Coherent Fresnel zone fields result in a spiky behavior in $\tilde{E}_z(x,z)$ near the apertures, which gives a small amount of numerical uncertainty in the first ~ 5 μm distance along the z axis from the aperture boundary. Our calculations, as shown in Fig. 4, give a 17% gain reduction for a 4 μm slit aperture, and a 34% gain reduction for a 6 μm one relative to the case of no aperture present.

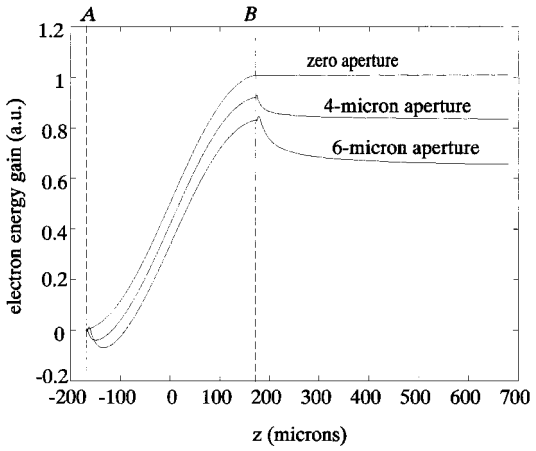

FIG. 4. Electron energy gain vs distance with no electron aperture, a 4 μm slit aperture, and a 6 μm slit aperture. The two dashed lines correspond to the two boundaries A and B in Fig. 1. The electron energy gain decreases 17% for the 4 μm slit aperture case, and decreases 34% for the 6 μm one relative to the zero aperture case.

IV. DISCUSSION

We have calculated the acceleration field in the proposed crossed-laser-beam linear accelerator with and without the presence of an electron transit aperture. In a laser-driven accelerator, the electron transit aperture, typically comparable or larger than the driving laser wavelength, may result in a nontrivial laser field leaking through the accelerator cell. The electron energy gain is reduced by 17% for a 4 μm electron aperture and by 34% for a 6 μm one relative to the case with no apertures.

ACKNOWLEDGMENTS

The work at National Tsinghua University, Taiwan, is supported by the National Science Council under Contract No. NSC-87-2112-M-007-024, and that at Stanford University is supported by the Department of Energy under Contract No. DE-AC03-76SF00515.

[1] Y. C. Huang, D. Zheng, W. M. Tulloch, and R. L. Byer, Appl. Phys. Lett. **68**, 753 (1996).
[2] Y. C. Huang and R. L. Byer, Appl. Phys. Lett. **69**, 2175 (1996).
[3] Y. C. Huang and R. L. Byer, Proceedings of the 18th Free-electron Laser Conference, edited by G. Dattoli and A. Renieri, Rome, Italy, Aug. 1996 (unpublished), p. II-37.
[4] J. A. Edighoffer and R. H. Pantell, J. Appl. Phys. **50**, 6120 (1979).
[5] C. M. Haaland, Opt. Commun. **114**, 280 (1995).
[6] P. Sprangle, E. Esarey, J. Krall, and A. Ting, Opt. Commun. **124**, 69 (1996).
[7] A. E. Siegman, *Lasers* (University Science Books, Mill Valley, CA, 1986), p. 646.
[8] A. E. Siegman, *Lasers* (University Science Books, Mill Valley, CA, 1986), p. 664.
[9] A. E. Siegman, *Lasers* (University Science Books, Mill Valley, CA, 1986), p. 682.
[10] M. O. Scully, Appl. Phys. B: Photophys. Laser Chem. **51**, 238 (1990).
[11] A. E. Siegman, *Lasers* (University Science Books, Mill Valley, CA, 1986), p. 670.
[12] B. C. Stuart, M. D. Feit, A. M. Rubenchik, B. W. Shore, and M. D. Perry, Phys. Rev. Lett. **74**, 2248 (1995).
[13] S. Silver, J. Opt. Soc. Am. **52**, 131 (1964).